Study of Li Diffusion on Metal and Semiconductor Surfaces via NQI

H. J. Jänsch

Fachbereich Physik and Wissenschaftliches Zentrum für Materialwissenschaften, Philipps-Universität, D-35032 Marburg

Reprint requests to H. J. J.; E-mail: heinz.jaensch@physik.uni-marburg.de

Z. Naturforsch. **55 a,** 15–20 (2000); received August 23, 1999

Presented at the XVth International Symposium on Nuclear Quadrupole Interactions, Leipzig, Germany, July 25 - 30, 1999.

Nuclear magnetic resonance has been used to study the diffusion of lithium on a Ru(001) single crystal surface. The quadrupolar interaction of the radioactive probe nucleus ^{8}Li was utilized for this. In an online experiment the ^{8}Li nuclei are produced, thermalized and highly polarized before they land on the surface studied, the parity violating β–decay revealing the sought after NMR/NQI nuclear information through the spatial asymmetry of the decay electrons. As a function of substrate temperature, alkali metal coverage and magnetic field the nuclear spin-lattice relaxation measurements show the existence of two distinctly different diffusion barriers on the surface, valued at 0.45 eV and 0.15 eV. The former is attributed to jumps from step to terrace sites, whereas the latter is the barrier between adjacent terrace sites. On the substrate Si(111)7x7 the relaxation measurements suggest a much higher diffusion barrier around 0.8 eV.

PACS: 68.35Fx, 76.60Es, 82.65M

Key words: Diffusion; Alkali Atom; Surfaces; NMR; NQI.

Diffusion of adsorbates constitutes one of the fundamental physical processes involved in many surface phenomena such as adsorption/desorption, catalytic reactions, growth or phase transitions. Compared to its importance, the amount of available experimental material and the insight in details of the mass transport process is rather low [1]. Due to the presence of steps, kinks, vacancy sites and the like on every real crystal surface a large variety of single jump processes exists on a microscopical scale besides the jumps between neighbouring terrace sites [2]. Especially these defect sites influence the above mentioned complex dynamical processes strongly.

In bulk physics many methods have been developed to study these phenomena through NMR or NQI. This is essentially impossible for surface problems do to the inherently low sensitivity of NMR techniques. On a single crystal surface of 1 cm^2 size about 10^{15} sites are present. Typically 10^{17} to 10^{19} equivalent sites must be present for solid state NMR experiments. In recent years experiments in the Marburg surface science group were developed to increase the sensitivity by 5 to 10 orders of magnitude, thus making NMR and NQI tools to investigate single crystal surfaces [3 - 6].

The low symmetry of a single crystal surface makes electric field gradients (EFGs) ever present phenomena. Quadrupolar nuclei experience these EFGs and through diffusion the atoms have different local environments, i. e. different EFGs. These fluctuations lead to spin lattice relaxation, which is observed through the ^{8}Li β–decay asymmetry. The temperature, magnetic field and coverage dependence of this relaxation rate is studied to extract the diffusion parameters. On the substrate ruthenium (Ru(001), hcp crystal structure) the temperatur dependence was analyzed in a Bloombergen, Percel, Pound[7] like model (BPP) and a diffusion barrier of 0.45 eV was found for low coverages [8]. At higher coverage another diffusion barrier becomes observable [8] and the coverage dependent measurements are analyzed in a Monte Carlo type random walk model. Newly available low temperature and high magnetic field data allows to determine the diffusion barrier and the preexponential. A much lower value of 0.146 eV is found for the barrier and a prefactor of 2×10^{12}/s [9]. The latter values are under-

0932–0784 / 00 / 0100–0015 $ 06.00

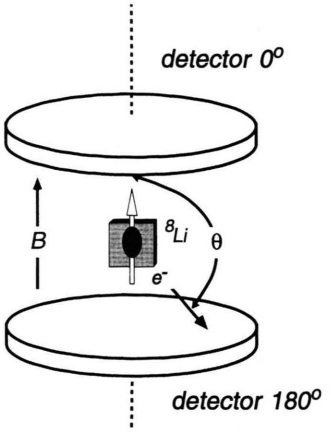

Fig. 1. The principle of β–NMR: The decay–electrons are emitted with a higher probability opposite to the direction of the nuclear spin. Therefore, the normalized asymmetry ϵ of the count rate N (0°) and N (180°) yields the polarization of the spin–ensemble.

stood as on–terrace diffusion, while the former is most likely the step–to–terrace barrier. On silicon (Si(111)-7x7) a much higher diffusion barrier for the lithium diffusion is found. The data being much more scarce, so a value around 0.8 eV is suggested.

The principle of the β–NMR experiments is shown in Figure 1. In the parity violating decay the electrons of ^{8}Li (nuclear spin I = 2, half-life = 0.84 s, endpoint energy 12.4 MeV) are emitted following the probability [10]

$$W(\theta) = W(90°)\,(1 + \frac{v}{c} A P \cos\theta) \qquad (1)$$

with θ being the angle between the magnetic field and the emission direction. The factor A is nuclear structure dependent and –1/3 in our case, the v/c can be set to 1. The longitudinal nuclear polarization P can be extracted by measuring the count rate asymmetry

$$\epsilon = \frac{N(0°) - N(180°)}{N(0°) + N(180°)} = -\frac{1}{3} P. \qquad (2)$$

Here $N(0°)$ and $N(180°)$ denote the count rate under $\theta = 0°$ and 180°, respectively. The decay of the polarization (P or ϵ) is described by a simple exponential:

$$P(t) = P(0)\, e^{-\alpha t} = P(0)\, e^{-t/T_1}. \qquad (3)$$

The T_1–times are the principle observables. They can be determined in the range 0.1 ... 10 half-life of ^{8}Li, thus giving a natural window for the isotope used.

Experimental

The experimental setup has been described in detail [5, 6]. A sketch of the most important components is given in Figure 2. The ^{8}Li isotope, we use, is produced in the nuclear reaction d(^{7}Li,^{8}Li)p from a 24 MeV $^7Li^{3+}$ ion beam. To ensure a gentle "landing" on the Ru(001) surface and not an implantation of the ^{8}Li the fast reaction product is thermalized by implanting it into a tubular graphite stopper, from which it is evaporated thermally. The thermal atomic beam thus formed is highly polarized by the application of laser optical pumping. A shutter ensures controlled timing of the atomic beam. A differential pumping section separates the beam production chamber from the NMR and surface analysis chamber. A magnetic field up to 0.9 T is provided by an electromagnet. Between the pole shoes and the chamber pairs of plastic szintillator detectors are placed on both sides. They are connected to light guides and photomultipliers to detect the decay electrons. The crystal can be positined into the center of the magnet or infront of several analytical tools by a manipulator, that also allows for heating and cooling (90 K up to 1500 K). A load lock can be used to introduce wet chemically prepared silicon crystals (Si(111) hydrogen terminated) into the chamber. The surfaces can be characterized by standart methods to ensure chemical cleanliness (Auger electron spectroscopy, AES) and structural integrity (low energy electron diffraction, LEED). Adsorbate coverage can be controlled by thermal desorption spectroscopy (TDS). The work-function change is monitored by a vibrating capacitor probe ($\Delta\Phi$).

The UHV chamber has a base pressure of 5×10^{-11} mbar. The crystal is cleaned using argon ion bombardment and prolonged heating in oxygen atmosphere (oxygen background 1×10^{-6} mbar at 1200 K) followed by a sequence of flashes and annealing. Additional lithium can be dosed onto the surface using thoroughly outgassed SAES dispenser sources. The Li dispensers are calibrated (achieved surface coverage vs. heating current and time) by multiple TDS experiments. 1 ML is defined as the complete coverage of the first layer, as seen in TDS experiments by the onset of the multilayer peak at 560 K [11, 12]. According to LEED–IV experiments 1 ML corresponds to Θ = 0.78 with respect to the number of Ru substrate atoms on the surface [13, 14].

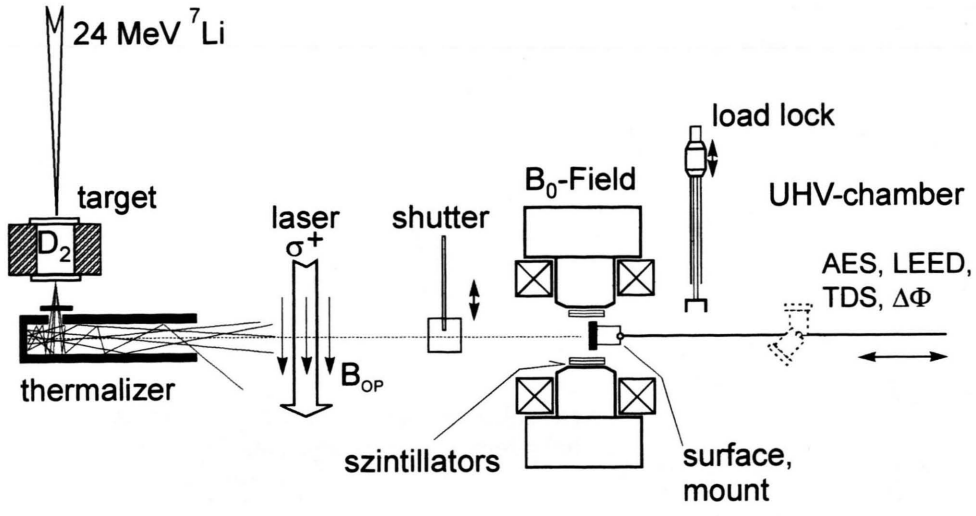

Fig. 2. Schematic view of the experimental setup. A description is given in the text.

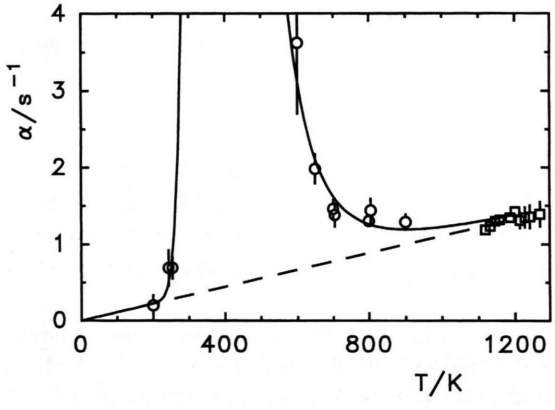

Fig. 3. The nuclear spin lattice relaxation rate α as a function of the surface temperature. The dashed line gives the Fermi contact part of the relaxation, whereas the solid line includes the diffusional relaxation.

Results and Discussion

Ru: Low Coverage

Figure 3 shows the nuclear spin relaxation (NSR) rates $\alpha = 1/T_1$ as a function of surface temperature in a wide range from 200 K to 1200 K. The surface is precovered with 0.02±0.01 ML of stable lithium to avoid the trapping of the very scarce ^{8}Li at rare surface sites [15, 16]. The relaxation rate starts to rise with increasing surface temperature and reaches a maximum between 300 and 500 K, where the measurement is virtually impossible. With a further increase of the surface temperature the NSR rates decrease strongly and approach a linear increase with temperatur. The peak–like structure is caused by diffusion of the lithium probe atoms, while the apparent underlying linear increase of the NSR rate with temperature is caused by interaction with the conduction electrons (Fermi contact interaction). Both relevant relaxation mechanisms are discussed below.

The linear contribution in Fig. 3 is caused by the "Fermi contact" interaction of the magnetic moments of the delocalized metal electrons with the nuclear moments (Korringa relaxation) [17, 18]. The rate bears information on the local density of states at the Fermi energy of the Li adsorbate [19]. The explicit form of the NSR rate has been derived for metallic bulk systems by Korringa for the first time [20] and also holds for surface adsorbates [21]

$$\alpha_K = \frac{256\pi^3}{9}\mu_e^2\left(\frac{\mu(^8\mathrm{Li})}{I}\right)^2 \mathrm{LDOS}(E_F)^2 \cdot \frac{kT}{\hbar}. \quad (4)$$

$\mu(^8\mathrm{Li})$ and μ_e denote the magnetic moments of the nucleus and the electron respectively, $\mathrm{LDOS}(E_F)$ is the local density of electronic s–states at the Fermi energy and at the position of the nucleus. The quantity is often written as $\mathrm{LDOS}(E_F)=\rho(E_F)\cdot|\Psi(0)|^2$. Experimentally a value of $0.13(\pm0.01)\ \mathrm{eV}^{-1}\mathrm{\AA}^{-3}$ can be determined, which compares well with two recent theoretical studies [24 - 24] for the low coverage regime.

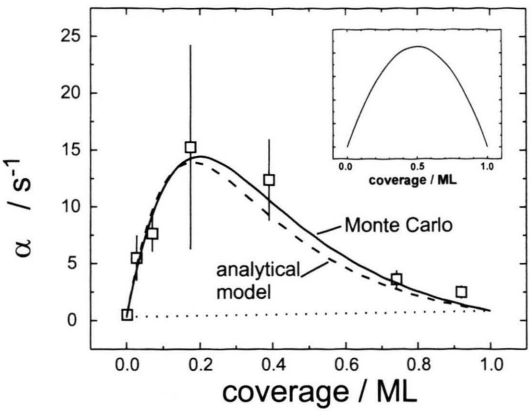

Fig. 4. Nuclear spin relaxation rates α as a function of Li coverage at a substrate temperature of 200 K. The solid line shows the results of a Monte Carlo simulation of the diffusion process taking the change of the dipole moment with coverage of the adsorbed Li (Fig. 5) into account. The insert displays a simulation without considering this change of the dipole moment.

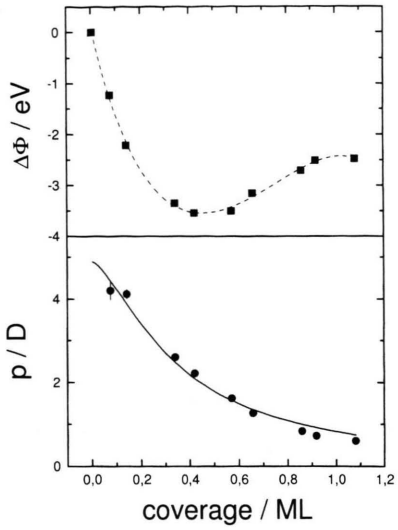

Fig. 5. As a function of Li coverage, change in the work function $\Delta\phi$ (upper figure) and the resulting dipole moment p per lithium atom (lower figure). The solid line in the lower spectrum is the result of fitting the Topping formula to the data, which takes into account the depolarization by the field of surrounding dipoles.

In Fig. 3 the strong increase of the relaxation rate between 300 and 600 K attributed to diffusion. Fluctuations of the interaction between the nuclear quadrupole moment of ^{8}Li[25] and the surrounding electric field gradient (EFG) lead to transitions between the spin substates and therefore the level populations can reach thermal equilibrium (nuclear spin relaxation) [17, 10, 18]. Such fluctuations are introduced by the atomic motion across the surface. Mathematically the Fourier transform of the autocorrelation function of the time dependent part of the Hamiltonian, i. e. the spectral density, gives the frequency spectrum of the field fluctuations. Evaluation of this spectrum at the resonance (Larmor) frequency ω_L of the nuclear spin gives the nuclear spin relaxation rate α [17]. This concept leads to a quasi–resonant temperature dependence of the relaxation rate, if one assumes that the correlation time τ_c is related to diffusion [10, 7] and thermally activated

$$\tau_c = \tau_0 \cdot \exp\left(E_{\mathrm{Diff}}/kT\right). \tag{5}$$

Here E_{Diff} denotes the diffusion energy and τ_0 a time prefactor. At low temperature the spectrum is restricted to frequencies below the Larmor frequency. At high temperature the spectrum extends over a vast frequency range with a low spectral density at ω_L. At an intermediate temperature ($\omega_L \cdot \tau_c \approx 1$) the spectral density and therefore the relaxation rate reaches a maximum. The solid line in Fig. 3 is a best fit resulting from an empirical model for the relaxation rate, which has been proven in two dimensional systems [26, 27]:

$$\alpha = G \cdot \tau_c \ln\left(1 + (\omega_L \cdot \tau_c)^{-2}\right). \tag{6}$$

G stands for the strength of the interaction of the nuclear moments with the local electric field gradient. Using these equations a diffusion energy of 0.45 eV is extracted. This value together with the Korringa relaxation is seen in Fig. 3 as the solid line, which describes the data very well. The high value of the diffusion barrier is ascribed (see below) to the binding energy of the adatom at an abundant surface defect site, which is most likely the step. Therefore the barrier is interpreted as the step–to–terrace barrier.

Ru: High Coverage

Figure 4 shows the relaxation data as a function of Li coverage at 200 K. It can be understood as the result of the ^{8}Li atoms diffusion on a flat surface terrace within the neighboring Li atoms. The latter cause an EFG at the ^{8}Li nucleus, the value of which fluctuates in time as a result of the diffusional motion. The size of the EFG can be derived from the strong electric

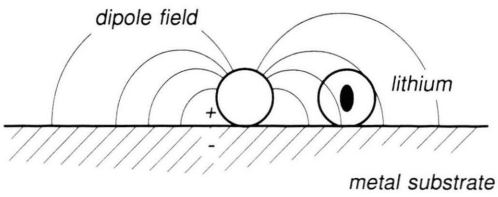

Fig. 6. Sketch of the electric field caused by the electric dipole moment of an adsorbed alkali metal atom. The nuclear quadrupole moment of a neighboring nucleus senses the resulting electric field gradient.

dipole moment each adsorbate carries. The workfunction change with alkali atom adsorption is caused by this. Figure 5 gives the workfunction change and the associated dipole moment. The EFG resulting from the dipole is schematically shown in Figure 6. In a Monte Carlo type treatment of the random motion of the surface atom within its environment, the time dependence to the EFG is determined. Here the diffusion is treated like in (5), that means the correlation time is taken from such an ansatz. The actual hopping time is assumed to be exponentially distributed. Site blocking is assumed. The power spectrum determined from such a model then determines the relaxation rate [8, 16]. The solid line in Fig. 4 is calculated in this manner. An analytical model was also developed, the central idea being that the fluctuations around the ^{8}Li atom is determined statistically [1] by $\Theta(1-\Theta)$ and the strength by the dipole moment squared $p(\Theta)^2$. The frequency dependence of the power spectrum is solely determined by the occurence of the diffusional jumps, thus introducing the temperature dependence as in (5). The result of the analytical model is also seen in Fig. 4 as a dashed line. Both models fit the data equally well. The analytical model can be easily used to fit data taken at different temperatures [9]. Using the data of Fig. 4 and values obtained at 105 K and 120 K, the diffusion parameters can be determined as $E_{\mathrm{Diff}} = 0.147$ eV and the prefactor as $\tau_0 = 2 \cdot 10^{-12}$s. These values are by virtue of the model the terrace diffusion parameters, therefore supporting the view that the 0.45 eV barrier is one belonging to an abundant trapping site.

A comparison to the literature is very difficult due to the scarcity of data. No other Li/Ru(001) diffusion study is known. Potassium has been studied by laser induced thermal desorption [28], a method that studies macroscopic diffusion by a refilling technique. The authors find diffusion energies between 0.32 to 0.36 eV. Given all the differences in the systems this is in reasonable agreement, since the macroscopic measurement cannot identify local barriers.

Si: Si(111)-7x7

The study of semiconductor surfaces with the ^{8}Li probe is still developing. Therefore only very preliminary information can be given. The relaxation rate shows no peak like structure up to 600 K. Only above this temperature the rate rises sharply to values that can only be determined with large error. If this rise in relaxation rate is due to diffusion, an estimate of a diffusion barrier can be given, which is about 0.8 eV [29]. The strong magnetic field dependence of this feature [30] supports the preliminary interpretation of the diffusional nature of the relaxation peak.

Acknowledgement

Special thanks are expressed towards the Max-Planck-Institut für Kernphysik for its generous handling of beam time requests and the continous support we received. The authors gratefully acknowledge the financial support through the Bundesministerium für Bildung und Forschung, Bonn, under various contracts.

[1] R. Gomer, Rep. Prog. Phys. **53**, 917 (1990).
[2] G. L. Kellogg, Surf. Sci. Rep. **21**, 1 (1994).
[3] H. Arnolds et al., Solid State Nuclear Magnetic Resonance **11**, 87 (1998).
[4] H. J. Jänsch, Appl. Phys. A **65**, 567 (1997).
[5] W. Widdra et al., Rev. Sci. Instrum. **66**, 2465 (1995).
[6] M. Detje et al., J. Vac. Sci. Technol. A **13**, 2532 (1995).
[7] N. Bloembergen, E. M. Purcell, and R. V. Pound, Phys. Rev. **73**, 679 (1948).
[8] H.-D. Ebinger et al., Phys. Rev. Lett. **76**, 656 (1996).
[9] G. Kirchner, Ph.D. thesis, Philipps–Universität, Marburg 1999.
[10] H. Ackermann, P. Heitjans, and H.-J. Stöckmann, in Hyperfine Interactions of Radioactive Nuclei, edited by J. Christiansen, Springer, Berlin 1983.
[11] D. L. Doering and S. Semancik, Surf. Sci. **175**, L730 (1986).

[12] H. J. Jänsch, C. Huang, A. Ludviksson, and R. M. Martin, Surf. Sci. **315**, 9 (1994).
[13] M. Gierer, H. Over, H. Bludau, and G. Ertl, Surf. Sci. **337**, 198 (1995).
[14] M. Gierer, H. Over, H. Bludau, and G. Ertl, Phys. Rev. B **52**, 2927 (1995).
[15] W. Preyß et al., Hyperfine Interactions **110**, 295 (1997).
[16] H. D. Ebinger et al., Surf. Sci. **412/413**, 586 (1998).
[17] C. P. Slichter, Principles of Magnetic Resonance, 3rd ed., Springer, Berlin 1989.
[18] A. Abragam, The Principles of Nuclear Magnetism, University Press, Oxford 1961.
[19] H. J. Jänsch et al., Phys. Rev. Lett. **75**, 120 (1995).
[20] J. Korringa, Physica **16**, 601 (1950).
[21] W. Mannstadt and G. Grawert, Phys. Rev. B **52**, 5343 (1995).
[22] W. Mannstadt and A. J. Freeman, Phys. Rev. B **57**, 13289 (1998).
[23] L. Hufnagel, Master's thesis, Philipps-Universität, Marburg 1998.
[24] L. Hufnagel, D. Fick, and M. Scheffler, to be published (1999).
[25] T. Minamisono et al., Phys. Rev. Lett. **69**, 2058 (1992).
[26] P. M. Richards, Solid State Comm. **25**, 1019 (1978).
[27] W. Küchler, P. Heitjans, A. Payer, and R. Schöllborn, Sol. State Ionics **70/71**, 434 (1994).
[28] E. D. Westre, D. E. Brown, J. Kutzner, and S. M. George, Surf. Sci. **294**, 185 (1993).
[29] H. Winnefeld, PhD Thesis, Marburg 1999, to be published.
[30] C. Weindel, PhD Thesis, Marburg 1999, to be published.